

Prognostic and functional role of hyaluronan-binding protein 1 in pancreatic ductal adenocarcinoma

YASUHIRO ADACHI¹, NORIHIRO SATO¹, TAKUYA OBA¹, TAKAO AMAIKE¹,
YUZAN KUDO¹, SHIRO KOHI¹, TOSHIYUKI NAKAYAMA² and KEIJI HIRATA¹

Departments of ¹Surgery I and ²Pathology, School of Medicine, University of Occupational and
Environmental Health, Kitakyushu, Fukuoka 807-8555, Japan

Received January 21, 2022; Accepted April 6, 2022

DOI: 10.3892/ol.2022.13343

Abstract. Hyaluronan-binding protein 1 (HABP1) is among the molecules known to bind to hyaluronan and is involved in a variety of cellular processes, including cell proliferation and migration. HABP1 has been implicated in the progression of various cancers; however, there have been (to the best of our knowledge) few studies on the expression and function of HABP1 in pancreatic ductal adenocarcinoma (PDAC), a topic that is examined in the present study. Immunohistochemical analysis of HABP1 protein was conducted in archival tissues from 105 patients with PDAC. Furthermore, the functional effect of HABP1 on proliferation, colony formation, and migration in PDAC cells was examined by knockdown of *HABP1*. It was revealed that HABP1 was overexpressed in 49 (46.2%) out of 105 patients with PDAC. Overall survival was significantly shorter in patients with high HABP1 expression than in those with low HABP1 expression (median survival time of 12.8 months vs. 28.5 months; log-rank test, $P=0.004$). Knockdown of *HABP1* expression in PDAC cells resulted in decreased cell proliferation, colony formation, and cell migration activity. Thus, HABP1 may serve as a prognostic factor in PDAC and may be of use as a novel therapeutic target.

Introduction

Pancreatic ductal adenocarcinoma (PDAC) is one of the most aggressive neoplasms, ranking fourth among the causes of cancer-related deaths in Western countries and Japan (1,2). Currently, multidisciplinary treatments such as surgery, chemotherapy, and radiotherapy are used to treat pancreatic cancer, but the survival outcome has not been significantly improved. In addition, only a limited number of patients with PDAC may benefit from new treatment modalities, including immune checkpoint inhibitors and precision medicine based on genome-wide molecular alterations. Therefore, it is necessary to seek novel therapeutic strategies based on improved understanding of the biological and molecular mechanisms underlying the aggressive progression of PDAC.

Recently, the focus of cancer research has shifted to the microenvironment surrounding cancer cells. PDAC typically consists of a dense stroma comprising various stromal cells and rich extracellular matrices (ECMs) (3). Hyaluronan (HA), a major component of the ECM, accumulates to high levels in the microenvironment surrounding various cancers, including PDAC, and serves an important role in a variety of cellular processes, including cell invasion, migration, and proliferation (4-10). In addition, low-molecular-weight HA (LMW-HA) has been reported to be more critical for cancer progression in terms of invasion and metastasis compared to high-molecular weight HA (HMW-HA) (11-14). In a previous study by the authors it was shown that the accumulation of LMW-HA is correlated with the motility of PDAC cells (4). HA, a large linear glycosaminoglycan weighing up to approximately 107 Da in its naïve form, is produced by hyaluronan synthase enzymes (HASs) and degraded into smaller fragments by hyaluronidases (HYALs). In another previous study, the authors reported that strong expression of HAS2 (one of the HAS proteins) in PDAC was associated with poor survival after surgery (15). Distinct from HA synthesis, HA degradation is implicated in cancer prognosis. Specifically, the cleavage of large HAs (by HYALs or other enzymes) to yield smaller HA fragments is also accelerated in malignant tumors (4,8,11,14). Notably, in a previous study by the authors, HYAL1 [also referred to as KIAA1199 and as cell migration-inducing protein (CEMIP)] was shown to be overexpressed in PDAC (16).

Correspondence to: Dr Norihiro Sato, Department of Surgery I, School of Medicine, University of Occupational and Environmental Health, 1-1 Iseigaoka, Yahatanisi-ku, Kitakyushu, Fukuoka 807-8555, Japan
E-mail: norisato@med.uoeh-u.ac.jp

Abbreviations: CA19-9, carbohydrate antigen 19-9; CEMIP, cell migration-inducing and hyaluronan-binding protein; ECM, extracellular matrix; gC1qR, globular head receptor for complement component 1q; HABP1, hyaluronan-binding protein 1; HMW-HA, high-molecular-weight hyaluronan; HA, hyaluronan; HAS, hyaluronan synthase; HPDE, human pancreatic duct epithelial; HYAL, hyaluronidase; IHC, immunohistochemistry; LMW-HA, low-molecular-weight hyaluronan; LN, lymph node; ROS, reactive oxygen species; PDAC, pancreatic ductal adenocarcinoma

Key words: HABP1, pancreatic cancer, hyaluronan

In the present study, focus was on hyaluronan-binding protein 1 (HABP1), one of the multiple known hyaluronan-binding proteins. HABP1 originally was designated globular head receptor for complement component 1q (gC1qR), based on its characterization as a protein that inhibits C1 activation. Aberrant expression and/or function of HABP1 has been reported in neurodegenerative diseases, impaired glucose tolerance, and cancer (17-26). Notably, HABP1 has been demonstrated to play an important role in cancer initiation and progression (27,28). However, there have been (to the best of our knowledge) few studies on the expression and role of HABP1 in PDAC (25). In the present study, the expression, clinicopathological significance, and biological function of HABP1 in pancreatic cancer were investigated.

Materials and methods

Patient demographics. This retrospective study included samples from 105 consecutive patients (61 men and 44 women) with PDAC who were admitted to the Department of Surgery I, School of Medicine, University of Occupational and Environmental Health (Kitakyushu, Japan) between 1994 and 2014. The inclusion criteria included patients i) aged 33-90 years, ii) without other organ metastasis by preoperative examination, iii) diagnosed as having resectable tumors, and iv) definitively diagnosed with PDAC by postoperative pathology. Exclusion criteria included cases with i) preoperative chemotherapy or radiation therapy, ii) distant metastasis or a second cancer, iii) multiple organ failure, iv) history of drug abuse or v) patients who were pregnant. Within one week before pancreatic surgery, all patients underwent a baseline assessment of white blood cell count and of serum levels of alanine aminotransferase, total bilirubin, albumin carcinoembryonic antigen (CEA), and carbohydrate antigen 19-9 (CA19-9). Additional intra- and peri-operative data including tumor diameter, surgery time, blood loss, tumor stage, lymph node (LN) metastasis, and arterial involvement were collected. PDAC tissues had been fixed, processed, sectioned at the time of operation. Patients were staged according to Union for International Cancer Control (UICC) criteria (8th edition) (29).

Immunohistochemistry (IHC). The present study used archival tissues obtained from 105 consecutive patients who underwent surgery at the Department of Surgery I, School of Medicine, University of Occupational and Environmental Health (Kitakyushu, Japan). Tissues were fixed in 10% formalin at room temperature for 24 h and cut to a 2- μ m thickness. After formalin fixation, the tissue was paraffin-embedded. Written informed consent was obtained from each patient prior to use of their specimens. The present study was approved by the Ethics Committee of the School of Medicine, University of Occupational and Environmental Health (approval no. H26-118).

Paraffin-embedded sections were dewaxed with xylene and gradually hydrated. Endogenous peroxidase activity had been blocked at room temperature by immersing the sections in 0.3% hydrogen peroxide in methanol for 30 min after antigen retrieval was performed by autoclaving in 10 mM citrate buffer (pH 6.0) for 10 min. Each section was additionally blocked using 10% normal rabbit serum (cat. np.424033; Nichirei

Biosciences, Inc.). Each section was incubated in a 1:100 dilution of anti-HABP1 antibody (monoclonal anti-C1QBP antibody produced in mouse; catalog no. WH0000708M1; Sigma-Aldrich; Merck KGaA) for 1 day at 4°C, prior to being treated with secondary antibody and biotin-streptavidin complex (424033; Nichirei Corporation) for 60 min each at room temperature. The resultant immunoreactions were visualized with diaminobenzidine (Dako; Agilent Technologies, Inc.) and the sections were counterstained with hematoxylin (Wako Pure Chemical).

As a negative control, immunostaining was performed ~5 times using normal pancreatic tissue 2-5 cm away from the cancer. In addition, since the positive control of the anti-HABP1 antibody used was the duodenum, a second negative control was created by immunostaining the duodenum, using a diluted solution [PBS (pH 7.4) containing 0.1% BSA] excluding the primary antibody. The total score for the IHC reaction was quantified based on a staining intensity grade in combination with a score representing the percentage of positive tumor cells. The first value, the staining intensity grade, was determined as follows: 0 (no staining), 1 (weak staining), 2 (moderate staining), and 3 (strong staining). The second value was determined based on the percentage (0 to 100%) extent of reactivity, which was scored as follows: 0 (no positive tumor cells), 1 ($\leq 10\%$), 2 (11-49%) and 3 ($\geq 50\%$) (30). Each case was scored independently by two investigators in a blinded manner. The total score for each section was calculated as the product of the staining grade (value of 0-3) and extent of reactivity (0-3), meaning that the total score ranged from 0-9. Total scores ≤ 4 were regarded as negative for expression, and the remainder were classified as positive for expression. For example, if the staining intensity was strong (3 points) and the staining area was $< 10\%$ (1 point), the final score was 3, and the sample was classified as negative for expression.

Cell culture and reagents. PDAC cell lines, PANC-1 (CRL-1469; American Type Culture Collection), and NOR-P1 (TKG 0630; Cell Resource Center for Biomedical Research, Institute of Development, Aging and Cancer, Tohoku University) were used, both of which in our laboratory collection were shown (in the present study) to exhibit strong HABP1 expression. As other PDAC cell lines, the strains ASPC-1, Bx-PC3, Capan-1, CFPAC-1 (ASPC-1; CRL-1682, BxPC-3; CRL-1687, Capan-1; HTB-79, and CFPAC-1; CRL-1918; American Type Culture Collection), KP-3 (JCRB0178.0; JRCB Cell Bank), MiaPaca-2 (CRL-1420; American Type Culture Collection), SUIT-2 (JCRB01094; JRCB Cell Bank) and SW-1990 (CRL-2172; American Type Culture Collection) were used due to their weak expression of HABP1. NOR-P1 is a pancreatic ductal adenocarcinoma cell line established by Sato *et al.* (31). NOR-P1 was also used in a previous study (4). Separately, an immortalized cell line derived from human pancreatic duct epithelial (HPDE) cells, was also employed; this cell line was a kind gift from Dr Tsao (University of Toronto, Toronto, Canada). The PDAC cell lines were maintained in RPMI-1640 medium supplemented with 10% fetal bovine serum (FBS) and 1% streptomycin and penicillin (all from Life Technologies; Thermo Fisher Scientific, Inc.). HPDE was maintained in HuMedia-KG2 (Kurabo Industries, Ltd.). All cell lines were grown at 37°C in a 5% CO₂ incubator.

siRNA knockdown of HABP1. The small interfering RNA (siRNA) used to target *HABP1* (ON-TARGETplus SMARTPool Human *HABP1*; cat. no. L-011225-01-0005) and the negative control siRNA (ON-TARGETplus Control siRNA non-Targeting siRNA #1; cat. no. D-001810-01-05) were purchased from Horizon; PerkinElmer Inc. *HABP1* used a mixture of four target sequences. The target sequences were as follows (*HABP1*: 5'-GCGAAAUAGUGCGGAAA G-3', 5'-CGCAAGGGCAGAAGGUUGA-3', 5'-UUUCGU GGUUGAAGUUAUA-3' and 5'-GAAGUUAGCUUUCAG UCCA-3'. The non-targeting siRNA (negative control) was 5'-UGGUUUACAUGUCGACUAA-3'. NOR-P1 and PANC-1 were transfected with 100 nM siRNA using DharmaFECT 1 Transfection Reagent (Horizon; PerkinElmer, Inc.) according to the manufacturer's instructions at 37°C for 48 h. After 48 h of treatment, the cells were used for further experiments.

Reverse transcription-quantitative polymerase chain reaction (RT-qPCR). Total RNA was isolated from cultured cells using the RNeasy Mini Kit (Qiagen GmbH) according to the manufacturer's protocol. First-strand cDNA was synthesized from 1.0 µg of total RNA using the SuperScript® VILO cDNA synthesis Kit and Master Mix (Thermo Fisher Scientific, Inc.) according to the manufacturer's instructions. Quantitative mRNA expression analysis of *HABP1* and a control house-keeping gene (*GAPDH*, encoding glyceraldehyde phosphate dehydrogenase) was performed using TaqMan® Gene Expression Assays and the StepOnePlus™ Real-Time PCR System (both from Thermo Fisher Scientific, Inc.) according to the manufacturer's instructions. The amplification program consisted of 10 min of activation at 95°C, and 40 cycles of melting at 95°C for 15 sec followed by annealing/elongation at 60°C for 2 min. The assay IDs for these genes were as follows: Hs00241825_m1 (*HABP1*) and Hs02758991_g1 (*GAPDH*). The following oligonucleotides were used for analyses: *HABP1* forward, 5'-CTGCACACCGACGGAGAC AA-3' and reverse, 5'-CATATAAGGCCAGTCCAAG-3'; *GAPDH* forward, 5'-CTCCTCCACCTTTGACGCTG-3' and reverse, 5'-AGGGGAGATTCAAGTGTGGTG-3'.

The relative quantification was determined based on the Cq values, obtained from the reactions for target genes and an internal control gene in each sample (32).

Cell proliferation assay. PDAC cells (1.0x10⁴/dish) treated with the siRNA targeting *HABP1* or with the negative control siRNA were incubated for 1, 3 and 5 days at 37°C; cell counts then were determined using 0.5% trypan blue staining at room temperature for 1 min. The cell number was measured using a LUNA™ automatic cell counter (Logos Biosystems).

Colony formation assay. Following treatment with siRNA, PDAC cells were harvested and counted. Consistent numbers of cells (100 cells/dish) from each group were seeded in dishes. Cells were grown for 14 days and colonies were fixed at room temperature for 30 min, with the addition of 1 ml/well 4% neutral formalin solution and stained with 1% aqueous solution at room temperature for 5 min. The number of colonies on each dish was then counted under a light microscope. A colony was defined as a group of >50 cells that was ≥3 mm in size when stained with crystal violet.

Migration assay. The migratory activity of cells was determined by a Transwell cell migration assay using cell culture inserts equipped with a filter membrane containing 8-µm pores (BD Biosciences). The lower chamber was filled with RPMI-1640 medium containing 10% FBS. The upper chamber was filled with 2.0x10⁴ cells (for PANC-1) or 5.0x10⁴ cells (for NOR-P1) in RPMI-1640 medium (without FBS). After 24 h of incubation at 37°C, the cells remaining on the upper side of the filters were removed. The cells on the bottom surface of the membrane were stained with hematoxylin and eosin at room temperature for 15 min. and the number of cells that had migrated to the bottom surface of the membrane were counted in five randomly selected fields from each sample using a light microscope (x200 magnification).

Western blot analysis. The cells were harvested and total protein was extracted with PRO-PREP protein extraction solution (iNtRON Biotechnology, Inc.). Total protein was quantified using Pierce™ Microplate BCA Protein Assay Kit (Thermo Fisher Scientific, Inc.). Each lane was mounted with 10 µl of solution adjusted to a total protein of 1 µg. Equal amounts of protein per lane were subjected to electrophoresis on a 12% Mini-PROTEAN Precast Gel (Bio-Rad Laboratories, Inc.) and transferred to a polyvinylidene fluoride (PVDF) membrane (ATTO Corporation). Membranes were blocked for 1 h with 3% bovine serum albumin (BSA; Sigma-Aldrich, Merck KGaA) in TBST buffer (Tris-buffered saline, pH 7.4, containing 0.1% Tween-20) at room temperature. Blocked membranes were then incubated overnight at 4°C with anti-*HABP1* antibody at a dilution of 1:200 (mouse monoclonal anti-C1QBP antibody; WH0000708M1; Sigma-Aldrich; Merck KGaA) and anti-β-actin at a dilution of 1:5,000 (mouse monoclonal anti-β-actin; 66009-1-Ig; ProteinTech Group, Inc.), followed by incubation for 1 h at room temperature with appropriate HRP-conjugated anti-mouse IgG secondary antibodies (cat. no. SA00001-1; ProteinTech Group, Inc.) at a dilution of 1:4,000. The proteins were visualized using an ECL Western Blotting Detection System (GE Healthcare).

Statistical analysis. Statistical analyses were performed using SPSS statistical software (version 25.0; IBM Corp.). Two-tailed chi-squared tests, Student's t-tests, and Mann-Whitney U tests were used for group comparisons. In the present study, Student's t-test was unpaired. Kaplan-Meier survival curves and log-rank tests were used for survival analysis. Prognostic factors were evaluated by univariate and multivariate analyses using Cox proportional hazard regression models. P<0.05 was considered to indicate a statistically significant difference.

Results

Immunohistochemical analysis and prognostic relevance of HABP1 levels in PDAC. In the present study, pancreatic cancer tissue from 105 patients, of which 44 were women, was assessed. The median age was 69 years (range, 33-90 years). PDAC was localized in the pancreas head in 64 cases and in the pancreas body or tail in 41 cases (Table I). All target patients underwent R0 resection surgeries.

Immunohistochemical analysis was used to determine the expression pattern of *HABP1* protein in the PDAC tissue samples. *HABP1* expression was negative or only slightly

Table I. Comparison of clinicopathological variables between patients with low HABP1 expression and those with high HABP1 expression.

Characteristics	Expression of HABP1		P-value
	Low (n=56)	High (n=49)	
Sex			0.559
Male	31	30	
Female	25	19	
Age, years			0.104
≤65	16	22	
>65	40	27	
Location			0.559
Head	34	30	
Body and tail	22	19	
Tumor marker			
CEA	2.6 (1.0-13.6)	2.8 (1.0-3.7)	0.565
CA19-9	63.8 (0.6-4610)	149.1 (3.0-3450)	0.402
UICC T			0.191
1	3	3	
2	7	1	
3	34	30	
4	12	15	
Tumor size (cm)	2.6 (0.6-7)	3.2 (0.6-8)	0.009 ^a
UICC N			0.566
0	24	16	
1	25	26	
2	7	7	
UICC M			0.533
0	55	49	
1	1	0	
UICC stage			0.201
I (A+B)	7	2	
II (A+B)	32	26	
III	16	21	
IV	1	0	
Vascular invasion			0.497
Negative	15	10	
Positive	41	39	
Perineural invasion			0.331
Negative	31	22	
Positive	25	27	
Histological grade			0.509
High	4	6	
Low	52	43	
Adjuvant chemotherapy			0.672
+	40	32	
-	16	16	

^aStatistically significant difference. HABP1, hyaluronan-binding protein 1; CEA, carcinoembryonic antigen; CA19-9, carbohydrate antigen 19-9; UICC, Union for International Cancer Control; T, tumor; N, node; M, metastasis.

positive (IHC scores 0-4) in normal pancreata, including ductal cells, acinar cells, and islet cells, whereas HABP1 was

highly expressed in some tumor cells. Staining was detected in the membrane and/or cytoplasm of the tumor cells (Fig. 1).

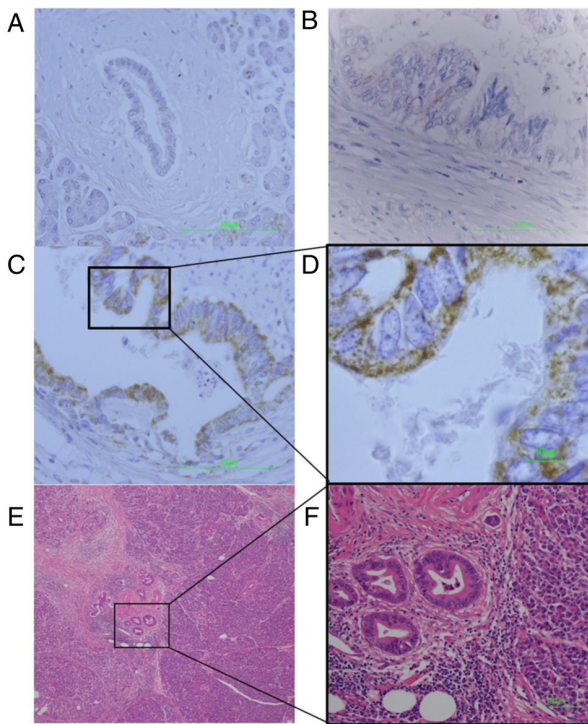


Figure 1. IHC of PDAC tissue observed by light microscope. (A) A normal pancreas, including ductal cells (magnification, x400; scale bar, 100 μ m). Normal pancreas staining was performed 5 times. (B) PDAC tissue exhibiting weak HABP1 staining (IHC score 1) (magnification, x400; scale bar, 100 μ m). (C) PDAC tissue exhibiting strong HABP1 staining (IHC score 9) (magnification, x400; scale bar, 100 μ m). (D) Magnified image of C (magnification, x1,000; scale bar, 10 μ m). HABP1 staining is observed in the membrane and/or cytoplasm of the tumor cells. (E) H&E-stained PDAC tissue. The PDAC portion of the specimen is located in the center of the micrograph, adjacent to normal pancreatic tissue (inset image). (F) H&E-stained PDAC tissue (magnification, x200; scale bar, 100 μ m). The PDAC cells forming the ductal structure exhibit a large nucleus-cytoplasm ratio and uneven distribution of nuclei. IHC, immunohistochemistry; PDAC, pancreatic ductal adenocarcinoma; HABP1, hyaluronan-binding protein 1; H&E, hematoxylin and eosin.

With regard to the 105 PDAC cases, 49 (46.7%) exhibited high HABP1 expression, whereas the remaining 56 (53.3%) exhibited low expression, according to our staining quantification criteria. Clinicopathological data were compared between the high-HABP1 expression group and low-HABP1 expression group (Table I). Analysis using Student's t-tests revealed that tumor size (tumor diameter) was significantly larger in the high-HABP1 expression group than in the low-HABP1 expression group [mean and range, 3.2 (0.6-8) vs. 2.7 (0.6-7) cm; $P=0.00883$]. There was no significant difference between the groups in other clinicopathological variables, including age, sex, tumor location, levels of tumor markers, UICC stage, as well as other pathological factors, as determined using analysis of two-tailed chi-squared tests, Student's t-tests, and Mann-Whitney U tests.

In the present study, the observation period was set to 5 years after surgery. The median survival time was 18.8 months (range, 3 to ≥ 60 months). The survival between the high- and low-HABP1 expression groups was then compared. The overall survival was significantly shorter in patients with high HABP1 expression (median survival time, 12.8 months) than in patients with low HABP1 expression (median survival

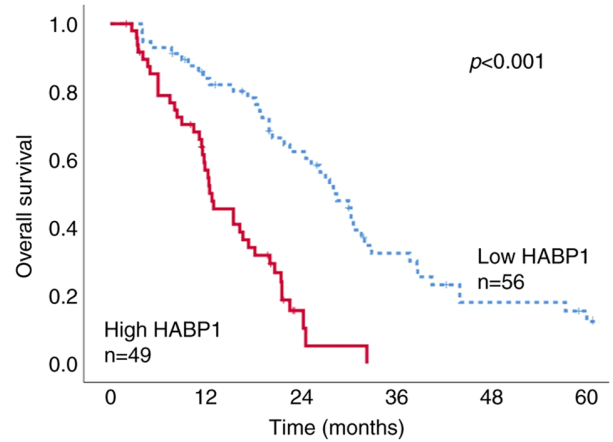


Figure 2. Kaplan-Meier survival curves for patients with PDAC exhibiting strong HABP1 expression and in those exhibiting weak HABP1 expression, as classified by immunohistochemical staining. PDAC, pancreatic ductal adenocarcinoma; HABP1, hyaluronan-binding protein 1.

time, 28.5 months) (log-rank test, $P<0.001$) (Kaplan-Meier survival curve; Fig. 2). In the present study, numerous patients succumbed to cancer metastasis in the HABP1-high expression group. In the high expression group, 35 out of 49 cases (71%) were reported as pancreatic cancer-associated deaths. In contrast, in the HABP1-low expression group, pancreatic cancer-related deaths were reported in 28 out of 56 (56%) cases (data not shown).

Prognostic factors were examined using Cox proportional hazard regression models. Multivariate analysis revealed high HABP1 expression ($P<0.001$), preoperative high CA19-9 levels ($P=0.031$), histological grade (high/low) ($P=0.046$), LN metastasis ($P=0.015$), and tumor stage ($P=0.013$) to be significantly associated with poor prognosis (Table II).

Functional analysis of HABP1 in PDAC cell lines. First, the mRNA expression of *HABP1* was investigated in a panel of 10 PDAC cell lines. *HABP1* mRNA was strongly expressed in 5 (50%) out of 10 PDAC cell lines investigated (compared with the level of expression in a control cell line, HPDE) (Fig. 3A). With regard to the cell lines with strong expression, two (NOR-P1 and PANC-1) were used for our subsequent experiments.

siRNA was used to knockdown *HABP1* expression in NOR-P1 and PANC-1 cells, two of the cell lines with strong *HABP1* mRNA expression. RT-qPCR revealed that transfection with the siRNA targeting *HABP1* (siRNA HABP1) resulted in a 97-99% decrease in *HABP1* mRNA levels in these cell lines (Fig. 3B and C). Western blot analysis validated the successful knockdown of *HABP1* expression at the protein level (Fig. 3D).

The proliferation, colony formation, and migration of NOR-P1 and PANC-1 cells with and without knockdown of *HABP1* were next examined; these experiments were expected to reveal aspects of the biological functions of HABP1 in pancreatic cancer. First, it was assessed whether *HABP1* knockdown affected PDAC cell proliferation. A cell counting assay revealed that the knockdown of *HABP1* significantly decreased the proliferation of PDAC cells compared with control cells on both days 3 and 5, using Student's t-tests

Table II. Univariate and multivariate analysis for factors predicting poor prognosis in patients with PDAC.

Characteristics	Univariate analysis			Multivariate analysis		
	HR	95% CI	P-value	HR	95% CI	P-value
<i>HABP1</i> (high/low)	1.995	1.537-2.591	<0.001 ^a	0.106	0.048-0.237	<0.001 ^a
Age	0.650	0.411-1.029	0.066	1.006	0.980-1.034	0.637
Sex (male/female)	1.153	0.734-1.798	0.529	0.890	0.482-1.644	0.710
Location (head/other)	1.304	0.836-2.035	0.242	0.635	0.342-1.180	0.151
Preoperative CEA	1.039	0.997-1.083	0.073	1.020	0.971-1.070	0.433
Preoperative CA 19-9	1.001	1.000-1.001	0.036 ^a	1.001	1.000-1.001	0.031 ^a
Histological grade (high/low)	1.196	0.610-2.345	0.602	0.358	0.130-0.980	0.046 ^a
Tumor size	1.255	1.098-1.434	<0.001 ^a	1.165	0.932-1.457	0.179
Lymph node metastasis	1.283	0.921-1.788	0.140	0.387	0.573-1.965	0.015 ^a
UICC stage (I/II/III/IV)	1.320	0.943-1.846	0.106	3.716	1.315-10.497	0.013 ^a
Vascular invasion (P/N)	1.301	0.789-2.145	0.302	1.084	0.530-2.216	0.826
Perinural invasion (P/N)	1.353	0.872-2.099	0.178	0.842	0.484-1.572	0.649
Adjuvant chemotherapy (±)	0.984	0.746-1.296	0.906	0.766	0.357-1.642	0.493

^aStatistically significant difference. *HABP1*, hyaluronan-binding protein 1; CEA, carcinoembryonic antigen; CA19-9, carbohydrate antigen 19-9; UICC, Union for International Cancer Control; P, positive; N, negative.

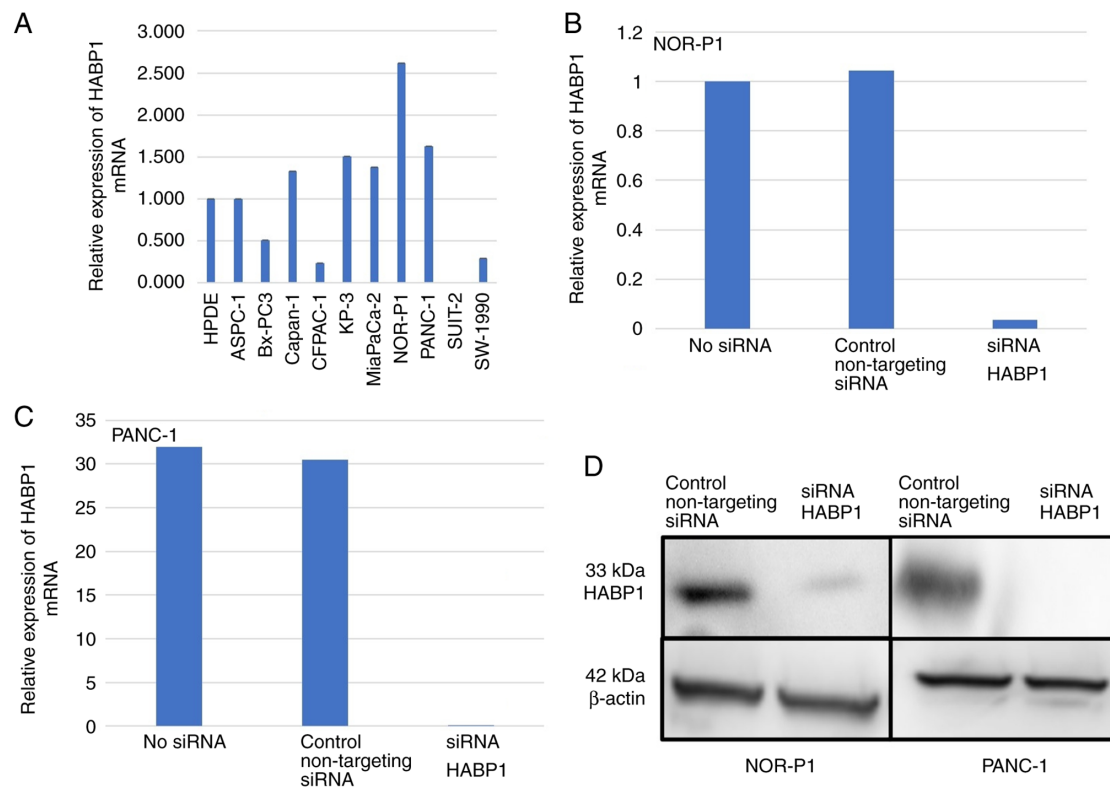


Figure 3. *HABP1* mRNA expression in PDAC cell lines and in cell lines in which *HABP1* was subjected to siRNA-mediated knockdown. (A) RT-qPCR showing *HABP1* mRNA expression in HPDE and 10 PDAC cell lines. The assay was performed twice. (B and C) RT-qPCR showing that transfection with siRNA targeting *HABP1* (siRNA *HABP1*) resulted in over 90% knockdown in both NOR-P1 and PANC-1 cell lines. The assay was performed twice. (D) Western blotting showing decreased *HABP1* protein levels in the knockdown groups. The images shown here are derived from a single experiment, for which the blots were processed in parallel. The assay was performed twice. *HABP1*, hyaluronan-binding protein 1; PDAC, pancreatic ductal adenocarcinoma; siRNA, small interfering RNA; RT-qPCR, reverse transcription-quantitative polymerase chain reaction; HPDE, human pancreatic duct epithelial.

(NOR-P1, $P < 0.001$; and PANC-1, $P < 0.001$; Fig. 4A). Next, it was revealed that the number of colonies was significantly decreased in the *HABP1*-knockdown cells compared with

the control cells for both cell lines (NOR-P1, $P = 0.011$; and PANC-1, $P = 0.038$; Fig. 4B). Finally, it was investigated whether *HABP1* affects cell migration. The Transwell migration assay

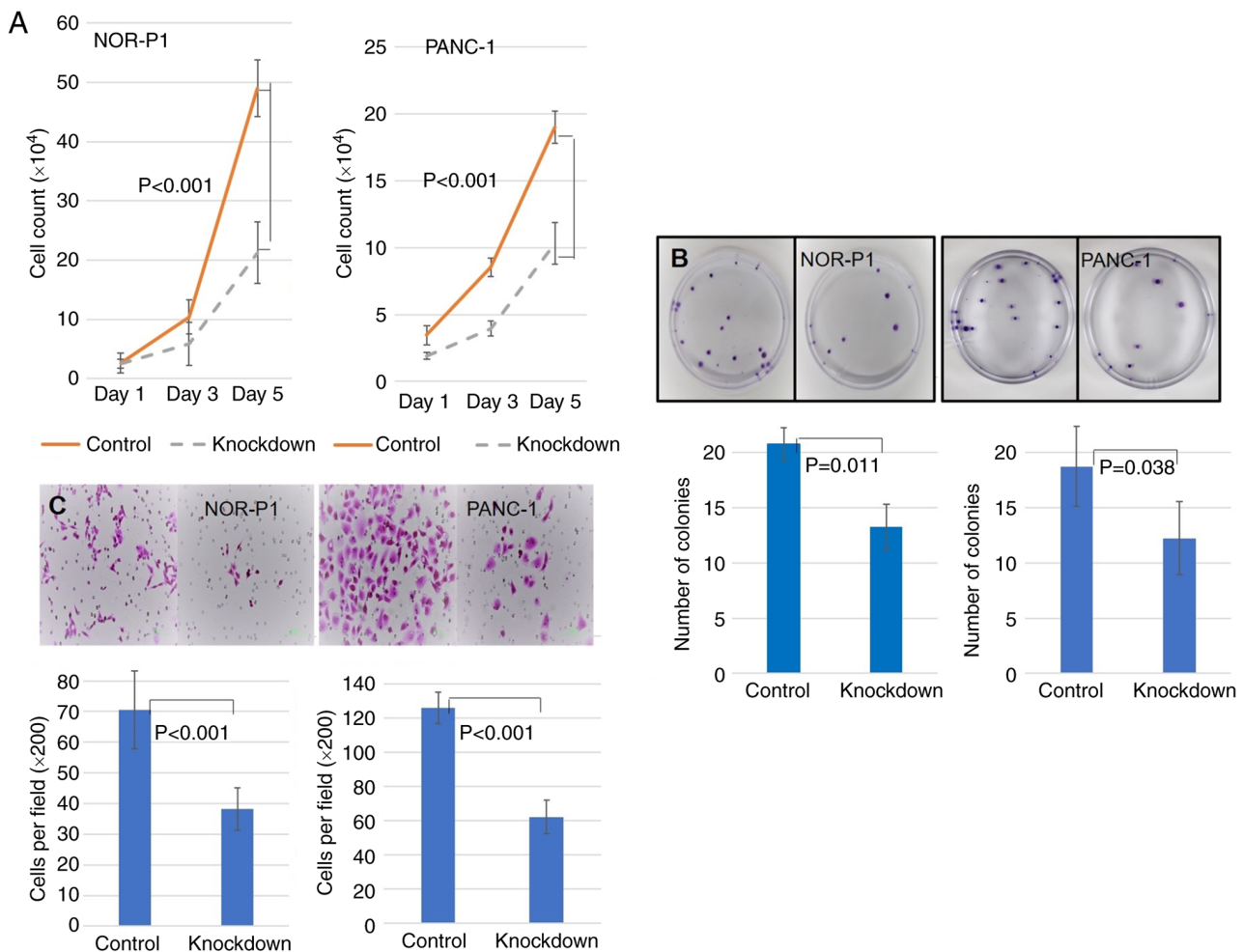


Figure 4. Knockdown of *HABP1* suppresses cell malignant behaviors. (A) At day 5, cell counts revealed that knockdown of *HABP1* resulted in a significantly decreased number of cells compared with the control, in both NOR-P1 and PANC-1 cells. Data are presented as the mean \pm SD (n=3). (B) Colony formation assays showing that *HABP1* knockdown resulted in a decreased number of colonies compared with the control. Data are presented as the mean \pm SD (n=3). (C) Migration assay showing that *HABP1* knockdown resulted in a decreased number of migrating cells compared with the control (n=5) (magnification x200). *HABP1*, hyaluronan-binding protein 1.

demonstrated that knockdown of *HABP1* significantly inhibited the migration of PDAC cells compared with the migratory activity of the control for both cell lines (NOR-P1, $P < 0.001$; and PANC-1, $P < 0.001$; Fig. 4C).

Discussion

In the present study, the expression and functional significance of *HABP1* in PDAC were investigated. The major findings obtained were as follows: i) *HABP1* protein was highly expressed in 49 (46.2%) out of 105 patients with PDAC; ii) the survival of patients with PDAC in which *HABP1* was strongly expressed was significantly shorter than in those with lower expression of *HABP1*; iii) multivariate analysis identified high *HABP1* expression as an independent factor predicting poor prognosis; and iv) knockdown of *HABP1* in PDAC cells resulted in decreased proliferation, colony formation, and migratory activities. Collectively, these findings suggest that *HABP1* may play a role in aggressive forms of PDAC.

HABP1 is a multi-functional glycoprotein ubiquitously expressed in various tissues. This protein has been shown to be involved in a variety of cellular processes, including cell

motility, senescence, apoptosis, and autophagy (24). Recently, it was revealed that *HABP1* overexpression triggers the induction of senescence in fibroblasts (33). These functions of *HABP1* demonstrate the important role of this protein in cancer initiation and progression. In fact, overexpression of *HABP1* in HepG2 cells was revealed to lead to enhanced cell survival and tumorigenicity by activating HA-mediated cell survival pathways (27,28). Similarly, exogenous administration of *HABP1* protein enhanced the migration and tumor growth of a melanoma cell line (34). However, the functional relevance of *HABP1* to PDAC remains unknown. In the present study, it was demonstrated, for the first time (to the best of our knowledge), that siRNA knockdown of *HABP1* impairs the proliferation, colony formation, and migration of PDAC cells. These findings suggest that *HABP1* is involved in the progression of PDAC, as well as in that of other cancer types.

It was also demonstrated that high *HABP1* expression was associated with shorter survival times in patients with PDAC who underwent surgery. Consistent with the results of the present study, it recently was reported that high cytoplasmic (but not nuclear) *HABP1* levels were strongly correlated with late tumor stages, arterial involvement, LN metastasis,

CA19-9 levels, and poor overall survival in patients with PDAC (25). It was also revealed, in the present study, that high HABP1 expression, as well as LN metastasis, tumor stage, and CA19-9 levels, were factors indicative of poor prognosis. The present study further suggested that histological grade was also an independent factor indicating poor prognosis. In cell experiments, knockdown of *HABP1* suppressed the malignant behaviors (such as the proliferation and migration activities) of PDAC cells. These results support the hypothesis that HABP1 is a prognostic factor for poor outcomes. In the immunohistochemical staining performed as part of this study, none of the 105 tested specimens demonstrated nuclear staining with the anti-HABP1 antibody, in contrast to the results reported by Xie *et al* (25). This difference most likely reflects the use of distinct antibodies. Nonetheless, the present results as well as those of Xie *et al* are in agreement with regard to the observation that the accumulation of HABP1 in the cytoplasm is an indicator of a poor prognosis. Since nuclear expression was not invoked as a prognostic factor in the study by Xie *et al*, it is proposed that the expression level of HABP1 in the cytoplasm is the critical characteristic detected by immunohistochemical staining for this protein. In other cancer types, including gastric, breast, and ovarian cancer, increased HABP1 expression levels were associated with worse patient outcomes (27,29,35-40). These findings suggest that HABP1 may be a promising prognostic marker in patients with PDAC and other cancers.

Regarding the therapeutic implications of the present, it was further inferred that HABP1 may be a promising therapeutic target for PDAC. Notably, high HABP1 expression was associated with improved survival of patients with malignant pleural mesothelioma who had received neoadjuvant or adjuvant chemotherapy (41). This result suggests that high HABP1 expression may serve as a biomarker in predicting the response to chemotherapy. In the present study, however, the association between high HABP1 expression and response to chemotherapy was unclear due to the limited number of patients. Further studies will be required to elucidate the relationship between HABP1 levels and chemosensitivity in PDAC.

The limitations of the present study were as follows. First, the study data lacked data on complications of patients with PDAC. Second, the study was a retrospective, single center study. Third, the study population was limited, rendering it difficult to draw a solid conclusion. Fourth, in our cohort of 105 patients with PDAC, some of the established prognostic factors, including adjuvant chemotherapy, did not demonstrate significant association with prognosis. Fifth, the number of cell experiments was not sufficient for statistical analysis in certain experiments. It is therefore inferred that our results may be biased due to the small sample size and long study period. Further investigations with larger and more-recent samples (for example, using tissue microarrays or data obtained by next-generation sequencing) would be required to confirm the results of the present study.

In conclusion, it was demonstrated that HABP1 accumulates to high levels in PDAC cells, and the expression of this protein is associated with prognosis. It was also determined that HABP1 is involved in the proliferation, colony formation, and migration of PDAC cells *in vitro*. These findings suggest that HABP1 may play a role in the progression of PDAC.

Acknowledgements

The authors would like to thank Ms Ueda (Department of Surgery I, University of Occupational and Environmental Health, Kitakyushu, Japan) for providing technical assistance.

Funding

The present research was funded by the University of Occupational and Environmental Health.

Availability of data and materials

The data that support the findings of this study are available (in anonymized form) from the corresponding author upon request.

Authors' contributions

YA conducted the molecular studies and drafted the manuscript. NS conceived the study, and participated in its design and coordination, and helped to draft the manuscript. TO, TA, YK SK, and TN participated in the molecular studies. KH participated in the design of the study. YA, NS and KH confirm the authenticity of all the raw data. All authors read and approved the final manuscript.

Ethics approval and consent to participate

The present study received ethical approval from the Ethics Committee of the University of Occupational and Environmental Health (Kitakyushu, Japan; approval no. H26-118). All patients provided written informed consent prior to specimen collection.

Patient consent for publication

Not applicable.

Competing interests

The authors declare that they have no competing interests.

References

1. Bray F, Ferlay J, Soerjomataram I, Siegel RL, Torre LA and Jemal A: Global cancer statistics 2018: GLOBOCAN estimates of incidence and mortality worldwide for 36 cancers in 185 countries. *CA Cancer J Clin* 68: 394-424, 2018.
2. National Cancer Center Japan: Cancer Registry and Statistics. Cancer Information Service. <https://ganjoho.jp/en/index.html>; Accessed 1 March, 2022.
3. Michl P and Gress TM: Improving drug delivery to pancreatic cancer: Breaching the stromal fortress by targeting hyaluronic acid. *Gut* 61: 1377-1379, 2012.
4. Cheng XB, Kohi S, Koga A, Hirata K and Sato N: Hyaluronan stimulates pancreatic cancer cell motility. *Oncotarget* 7: 4829-4840, 2016.
5. Itano N, Zhuo L and Kimata K: Impact of the hyaluronan-rich tumor microenvironment on cancer initiation and progression. *Cancer Sci* 99: 1720-1725, 2008.
6. Jacobetz MA, Chan DS, Neesse A, Bapiro TE, Cook N, Frese KK, Feig C, Nakagawa T, Caldwell ME, Zecchini HI, *et al*: Hyaluronan impairs vascular function and drug delivery in a mouse model of pancreatic cancer. *Gut* 62: 112-120, 2013.

7. Provenzano PP, Cuevas C, Chang AE, Goel VK, Von Hoff DD and Hingorani SR: Enzymatic targeting of the stroma ablates physical barriers to treatment of pancreatic ductal adenocarcinoma. *Cancer Cell* 21: 418-429, 2012.
8. Sato N, Kohi S, Hirata K and Goggins M: Role of hyaluronan in pancreatic cancer biology and therapy: Once again in the spotlight. *Cancer Sci* 107: 569-575, 2016.
9. Sironen RK, Tammi M, Tammi R, Auvinen PK, Anttila M and Kosma VM: Hyaluronan in human malignancies. *Exp Cell Res* 317: 383-391, 2011.
10. Toole BP, Wight TN and Tammi MI: Hyaluronan-cell interactions in cancer and vascular disease. *J Biol Chem* 277: 4593-4596, 2002.
11. Du Y, Cao M, Liu Y, He Y, Yang C, Wu M, Zhang G and Gao F: Low-molecular-weight hyaluronan (LMW-HA) accelerates lymph node metastasis of melanoma cells by inducing disruption of lymphatic intercellular adhesion. *Oncoimmunology* 5: e1232235, 2016.
12. Liu M, Tolg C and Turley E: Dissecting the dual nature of hyaluronan in the tumor microenvironment. *Front Immunol* 10: 947, 2019.
13. Sugahara KN, Hirata T, Hayasaka H, Stern R, Murai T and Miyasaka M: Tumor cells enhance their own CD44 cleavage and motility by generating hyaluronan fragments. *J Biol Chem* 281: 5861-5868, 2006.
14. Wu M, Cao M, He Y, Liu Y, Yang C, Du Y, Wang W and Gao F: A novel role of low molecular weight hyaluronan in breast cancer metastasis. *FASEB J* 29: 1290-1298, 2015.
15. Cheng XB, Sato N, Kohi S and Yamaguchi K: Prognostic impact of hyaluronan and its regulators in pancreatic ductal adenocarcinoma. *PLoS One* 8: e80765, 2013.
16. Kohi S, Sato N, Cheng XB, Koga A and Hirata K: Increased expression of HYAL1 in pancreatic ductal adenocarcinoma. *Pancreas* 45: 1467-1473, 2016.
17. Chowdhury AR, Ghosh I and Datta K: Excessive reactive oxygen species induces apoptosis in fibroblasts: Role of mitochondrially accumulated hyaluronic acid binding protein 1 (HABP1/p32/gC1qR). *Exp Cell Res* 314: 651-667, 2008.
18. D'Souza M and Datta K: A novel glycoprotein that binds to hyaluronic acid. *Biochem Int* 13: 79-88, 1986.
19. Li K, Gao B, Li J, Chen H, Li Y, Wei Y, Gong D, Gao J, Zhang J, Tan W, *et al*: ZNF32 protects against oxidative stress-induced apoptosis by modulating C1QBP transcription. *Oncotarget* 6: 38107-38126, 2015.
20. Li Y, Wan OW, Xie W and Chung KK: p32 regulates mitochondrial morphology and dynamics through Parkin. *Neuroscience* 199: 346-358, 2011.
21. Liu Y, Leslie PL, Jin A, Itahana K, Graves LM and Zhang Y: p32 heterozygosity protects against age- and diet-induced obesity by increasing energy expenditure. *Sci Rep* 7: 5754, 2017.
22. Liu Y, Leslie PL, Jin A, Itahana K, Graves LM and Zhang Y: p32 regulates ER stress and lipid homeostasis by down-regulating GCS1 expression. *FASEB J* 32: 3892-3902, 2018.
23. Muta T, Kang D, Kitajima S, Fujiwara T and Hamasaki N: p32 protein, a splicing factor 2-associated protein, is localized in mitochondrial matrix and is functionally important in maintaining oxidative phosphorylation. *J Biol Chem* 272: 24363-24370, 1997.
24. Saha P and Datta K: Multi-functional, multicompartmental hyaluronan-binding protein 1 (HABP1/p32/gC1qR): Implication in cancer progression and metastasis. *Oncotarget* 9: 10784-10807, 2018.
25. Xie ZB, Yao L, Jin C, Zhang YF and Fu DL: High cytoplasm HABP1 expression as a predictor of poor survival and late tumor stage in pancreatic ductal adenocarcinoma patients. *Eur J Surg Oncol* 45: 207-212, 2019.
26. Yagi M, Uchiyama T, Takazaki S, Okuno B, Nomura M, Yoshida S, Kanki T and Kang D: p32/gC1qR is indispensable for fetal development and mitochondrial translation: Importance of its RNA-binding ability. *Nucleic Acids Res* 40: 9717-9737, 2012.
27. Kaul R, Saha P, Saradhi M, Prasad RL, Chatterjee S, Ghosh I, Tyagi RK and Datta K: Overexpression of hyaluronan-binding protein 1 (HABP1/p32/gC1qR) in HepG2 cells leads to increased hyaluronan synthesis and cell proliferation by up-regulation of cyclin D1 in AKT-dependent pathway. *J Biol Chem* 287: 19750-19764, 2012.
28. Saha P, Ghosh I and Datta K: Increased hyaluronan levels in HABP1/p32/gC1qR overexpressing HepG2 cells inhibit autophagic vacuolation regulating tumor potency. *PLoS One* 9: e103208, 2014.
29. Brierley JD, Gospodarowicz MK and Wittekind C: TNM classification of malignant tumours. 8th edition. John Wiley & Sons, 2017.
30. Wang J, Song Y, Liu T, Shi Q, Zhong Z, Wei W, Huang S and Pang D: Elevated expression of HABP1 is a novel prognostic indicator in triple-negative breast cancers. *Tumour Biol* 36: 4793-4799, 2015.
31. Sato N, Mizumoto K, Beppu K, Maehara N, Kusumoto M, Nabae T, Morisaki T, Katano M and Tanaka M: Establishment of a new human pancreatic cancer cell line, NOR-P1, with high angiogenic activity and metastatic potential. *Cancer Lett* 155: 153-161, 2000.
32. Livak KJ and Schmittgen TD: Analysis of relative gene expression data using real-time quantitative PCR and the 2(-Delta Delta C(T)) method. *Methods* 25: 402-408, 2001.
33. Vikramdeo KS, Saha P, Dutta S, Kumar N, Roy Chowdhury A, Kumar S, Tyagi RK, Ghosh I and Datta K: Hyaluronan-binding protein 1 (HABP1) overexpression triggers induction of senescence in fibroblasts cells. *Cell Biol Int* 44: 1312-1330, 2020.
34. Prakash M, Kale S, Ghosh I, Kundu GC and Datta K: Hyaluronan-binding protein 1 (HABP1/p32/gC1qR) induces melanoma cell migration and tumor growth by NF-kappaB dependent MMP-2 activation through integrin alpha(v)beta(3) interaction. *Cell Signal* 23: 1563-1577, 2011.
35. Niu M, Sun S, Zhang G, Zhao Y, Pang D and Chen Y: Elevated expression of HABP1 is correlated with metastasis and poor survival in breast cancer patients. *Am J Cancer Res* 5: 1190-1198, 2015.
36. Yu H, Liu Q, Xin T, Xing L, Dong G, Jiang Q, Lv Y, Song X, Teng C, Huang D, *et al*: Elevated expression of hyaluronic acid binding protein 1 (HABP1)/P32/C1QBP is a novel indicator for lymph node and peritoneal metastasis of epithelial ovarian cancer patients. *Tumour Biol* 34: 3981-3987, 2013.
37. Gao H, Yao Q, Lan X, Li S, Wu J, Zeng G and Xue Y: Elevated HABP1 protein expression correlates with progression and poor survival in patients with gastric cancer. *Onco Targets Ther* 9: 6711-6718, 2016.
38. Zhang M, Li N, Liang Y, Liu J, Zhou Y and Liu C: Hyaluronic acid binding protein 1 overexpression is an indicator for disease-free survival in cervical cancer. *Int J Clin Oncol* 22: 347-352, 2017.
39. Jiang Y, Wu H, Liu J, Chen Y, Xie J, Zhao Y and Pang D: Increased breast cancer risk with HABP1/p32/gC1qR genetic polymorphism rs2285747 and its upregulation in northern Chinese women. *Oncotarget* 8: 13932-13941, 2017.
40. Zhao J, Liu T, Yu G and Wang J: Overexpression of HABP1 correlated with clinicopathological characteristics and unfavorable prognosis in endometrial cancer. *Tumour Biol* 36: 1299-1306, 2015.
41. Li X, Eguchi T, Aly RG, Chintala NK, Tan KS, Zauderer MG, Dembitzer FR, Beasley MB, Ghebrehiwet B, Adusumilli PS and Peerschke EIB: Globular C1q receptor (gC1qR/p32/HABP1) is overexpressed in malignant pleural mesothelioma and is associated with increased survival in surgical patients treated with chemotherapy. *Front Oncol* 9: 1042, 2019.



This work is licensed under a Creative Commons Attribution-NonCommercial-NoDerivatives 4.0 International (CC BY-NC-ND 4.0) License.